

On the Weaknesses of Backdoor-based Model Watermarks: An Information-theoretic Perspective

Aoting Hu, Yanzhi Chen, Renjie Xie, Adrian Weller

Abstract—Safeguarding the intellectual property of machine learning models has emerged as a pressing concern in AI security. Model watermarking is a powerful technique for protecting ownership of machine learning models, yet its reliability has been recently challenged by recent watermark removal attacks. In this work, we investigate why existing watermark embedding techniques particularly those based on backdooring are vulnerable. Through an information-theoretic analysis, we show that the resilience of watermarking against erasure attacks hinges on the choice of trigger-set samples, where current uses of out-distribution trigger-set are inherently vulnerable to white-box adversaries. Based on this discovery, we propose a novel model watermarking scheme, In-distribution Watermark Embedding (IWE), to overcome the limitations of existing method. To further minimise the gap to clean models, we analyze the role of logits as watermark information carriers and propose a new approach to better conceal watermark information within the logits. Experiments on real-world datasets including CIFAR-100 and Caltech-101 demonstrate that our method robustly defends against various adversaries with negligible accuracy loss ($\leq 0.1\%$)¹.

Index Terms—Model watermarking, Knowledge distillation, Intellectual property protection, Backdoor, Information theory

I. INTRODUCTION

TRAINING modern machine learning models often requires significant computational resources and access to a large, privately annotated dataset [1]. For example, the performance of the GPT-3 language model exhibits a power-law relationship with factors such as model size, dataset size, and computational capacity [2], [3]. Given the considerable expenses associated with this endeavor, owners of such models are usually highly motivated to safeguard their intellectual property (IP) [4]–[6].

The escalating threat of model theft intensifies the urgency of model copyright protection. The model stealing adversaries who possess black-box access to the victim model and a small part of unlabeled data can train a substitute model using the victim model’s predictions as supervision. The substitute model is designed to functionally mimic the behavior of the victim model. Representative works in this field include [7]–[9]. With the endorsement of model theft attacks, it enables the white-boxing of many other attacks, posing a significant threat to model security and privacy protection.

A. Hu is with the Anhui University of Technology, Maanshan 243002, China (email: aotinghu@ahut.edu.cn).

Y. Chen is with University of Cambridge and Microsoft Research, Cambridgeshire, CB2 1TN (email: yc514@cam.ac.uk).

R. Xie is with Nanjing University of Posts & Telecommunications, Nanjing 210003, China (e-mail: renjie_xie@njupt.edu.cn).

A. Weller is with University of Cambridge and Alan Turing Institute, Cambridgeshire, CB2 1TN (email: aw665@cam.ac.uk)

¹Under review. Code link: <https://github.com/Katerina828/IWE>

Watermark embedding (WE) is a powerful technique for protecting the copyright of machine learning models [10]–[12]. Originally used to protect the copyright of digital multimedia, WE works by hiding some secret information in the trained model [13], [14]. This secret information can be used later to verify the ownership of a model when copyright violation is suspected. Popular methods for implementing WE include either directly embedding the secret information into the parameters of the model [15]–[17] or by backdooring the model [16], [18]–[24]. The former method works by modifying the weights/biases of a DNN whereas the latter methods works by making the model highly predictive on some secret dataset (i.e., the trigger set) [18], [25], [26]. The latter methods can also be seen as utilizing the overfitting ability of modern machine learning models (e.g., a deep neural network) to memorize concealed patterns that are unlikely to be triggered by normal samples. Compared to methods that directly embed watermark information into the model parameters, backdoor-based methods are more light-weighted as they only need to examine the model output rather than the whole model during ownership verification, thereby have increasingly attracted much attention among the community.

One important question in model WE is how to establish a strong defense against potential adversaries. These adversaries are often aware of the existence of embedded watermark and may possess full knowledge about the technical details of the underlying watermark embedding schemes. They may even have partial or full access of the model parameters and are dedicated to remove the watermark embedded in the model by all means. In fact, most of the backdoor-based WE schemes have been proven ineffective in the presence of subsequent carefully-designed attacks [22], [27]–[34], especially when the model parameters are revealed [28]. One intuitive understanding of the vulnerability of backdoor-based methods is that these methods often rely on overfitting a specific dataset (i.e., the trigger set), which is fragile and can be easily overridden (by e.g., fine-tuning the model or knowledge distillation).

In this work, we aim to address the above threats of watermark erasure attacks by exploring two research questions: (a) why existing model watermarking schemes are susceptible to watermark erasure attacks; and (b) how to develop new watermark embedding schemes to overcome the limitation of existing schemes while maintaining utility. Our key insight is the vulnerability of existing watermark embedding schemes mainly comes from overfitting out-distribution trigger set samples, that *if there is no overlapping between normal samples and trigger set samples, the adversary can easily remove watermark without affecting model utility*. Only an appropriate

level of overlapping between these two sets of samples can guarantee the robustness of the watermarks. This vulnerability is fundamental and is well-grounded by information theory.

Motivated by this information-theoretic insight, we propose a new watermark embedding method, *in-distribution watermark embedding* (IWE), where the trigger set is designed to have a proper level of overlap with normal samples. This design encourages that the patterns learned for the main task (which classifies normal samples) and the watermark task (which classifies trigger set samples) are intricately entangled with each other, so that any attempts to remove the watermark will inevitably cause a degradation in main task performance. Notably, while prior arts [21], [35], [36] have also recognized the importance of entangling the main task and the watermark task, we offer a new perspective based on information theory, which is more principled and allows us to identify the suboptimality of these existing methods.

In addition to analyzing the choice of trigger set, we systematically explore how watermark information propagates within a watermarked model. This analysis crucially identifies redundant logits as a more suitable carrier for watermark information, which can in essence convey richer information than model predictions alone. By strategically utilizing these redundant logits, we can embed substantial information about model ownership without compromising the clarity of the main task predictions. This approach effectively minimizes potential conflicts between the main and watermark tasks, thereby rendering a minimal impact on performance.

We evaluated our method using three real-world datasets against five distinct types of adversaries, including two black-box adversary [7], [35] and three white-box adversaries [27]–[29]. Our experiments demonstrate that our method provides robust protection against all tested adversaries with only a negligible accuracy drop (within 0.1%), surpassing many existing watermarking schemes that are either susceptible to watermark removal attacks or experience significant performance declines. In addition to these established adversaries, we conducted a security analysis to address threats from potential adaptive adversaries, complemented by a discussion of our limitation.

To summarize, our main contributions are as follows:

- We provide a new information-theoretic perspective for understanding the limitation of existing backdoor-based WE method, explaining why these methods are intrinsically vulnerable in the presence of watermark erasure attacks;
- We develop a new watermark embedding scheme, named IWE, to provide a strong defense against watermark erasure attacks. Our method does not suffer from the same issue as existing methods;
- We evaluate our method on three real-world datasets, demonstrating its effectiveness against diverse adversaries. Only tiny performance drop ($\leq 0.1\%$) is observed.

The rest of this paper is organized as follows. Section II formulate the watermark embedding problem. Section III provide information-theoretic perspective for watermark embedding. Section IV and Section V elaborates the details of the In-distribution Watermark Embedding (IWE) and the corresponding watermark verification method. Section VI

TABLE I: Summary of Notations

Symbol	Description	Symbol	Description
X	Input variable	Y	label variable
x	Instance of X	y	Instance of Y
D	Train set	T	Trigger set
f	DNN models	f^*	Stolen DNN models
I	Mutual information	$\mathbf{1}$	Indicator function
\mathcal{L}_{CE}	cross-entropy loss	\hat{Y}	Prediction to Y
\mathcal{A}	Attacking algorithm	\mathcal{K}	Partition key
\mathcal{E}	Embedding algorithm	\mathcal{V}	Verification algorithm

present a detailed theoretical security analysis. Section VII show the experimental results and comprehensive comparison. Finally, Section VIII concludes this paper.

II. PROBLEM FORMULATION

A. Notations

Throughout this work, we focus on classification problem, where we denote the input data as X , the label as Y and the model as f . In this setting, the model $f : \mathbb{R}^N \rightarrow \mathbb{R}^K$ maps the input $X \in \mathbb{R}^N$ to a vector of prediction logits $f(X) = [f_1(X), f_2(X), \dots, f_K(X)]$ where the subscript is used to denote the position of the element, and the prediction is done by taking $\hat{Y} = \arg \max_i f_i(X)$. We use upper case characters (e.g., X) for random variables and lower case ones (e.g., x) for instances. Superscripts on instances indicate the instance number. For instance, $x^{(i)}$ denotes i -the input sample.

B. Threat Model

In this work, we consider a threat model with three parties: model owner, authority and adversary.

Model owner. This party develops the deep neural networks and would like to protect the intellectual property of the model using some watermarking mechanism. The model owner holds dataset D and a secret credit T associated with the watermark embedding process $\mathcal{E}(D, T)$. Following Kerckhoffs' Principle, the credit T should be kept secret from potential adversaries, akin to the secret key in a cryptographic system.

Authority. This party is a trusted third party (e.g., the government) responsible for verifying the ownership of a suspected model. In particular, the authority runs an verification algorithm $\mathcal{V}(f, T)$ to determine whether a suspect model f matches with the credit provided by a party. In this work, we assume that \mathcal{V} works in *grey-box* fashion where the authority verify model ownership by only inspecting the exposed model outputs, but reserve the rights to check the full details of the computational graph of the model.

Adversary. This party is a malicious user aiming to steal a model f or evade tracking using an attacking algorithm $\mathcal{A}(f)$. Depending on their knowledge, an adversary may have either (1) black-box access, knowing only the model's output (predictions), or (2) white-box access, knowing both the model parameters and architecture. The adversary may also possess a small fraction of auxiliary data D_{aux} drawn from the same distribution as the training data D . Additionally, we assume adversaries are aware of the existence of potential watermarks

TABLE II: Summary of watermark removal attacks. Here f and f^* are the models before and after removal, respectively.

	Knowledge Distillation [35]	Fine-tuning [28]	Model Pruning [27], [29]
Model access	black-box	white-box	white-box
Data access	subset of (un)labeled in-dist. data	subset of labeled in-dist. data	subset of labeled in-dist. data
Works by	aligning the logits of f and f^* by minimizing: $\lambda \mathcal{L}_{\text{CE}}(f^*(X), Y) + (1 - \lambda) \mathcal{L}_{\text{CE}}(f^*(X), f(X))$	fine-tuning f by well-chosen lr η' : $f^* \leftarrow f - \eta' \nabla_f \mathcal{L}_{\text{CE}}(f(X), Y), \eta' > \eta$	pruning weights \mathbf{w} in f : $\mathbf{w}^* = \mathbf{m} \odot \mathbf{w}$ where $m_i \in \{0, 1\}$

as well as the full knowledge about the details of the watermark embedding algorithm, except for the secret credit T . They may use these knowledge to erase any potential watermark embedded in the model.

C. Backdoor-based Model Watermarking

The goal of model watermarking is to let model owner embed secret information into the DNN models, which can be verified by a trusted third party later to help claiming model ownership. An effective model watermarking method should satisfy the following two properties simultaneously:

- *Fidelity*: the watermark embedding scheme does not impair the utility (i.e. prediction accuracy) of the protected model.
- *Robustness*: the embedded watermark is robust against watermark erasure attacks such as knowledge distillation, fine-tuning and model pruning.

Typically, a model watermarking system involves two processes:

Watermark embedding. In this stage, the model owner train the model with private database $D = \{x^{(i)}, y^{(i)}\}_{i=1}^n$ and incorporates credit T into the model f , represented as

$$\mathcal{E}(D, T) \rightarrow f. \quad (1)$$

Various approaches have been developed to realize this goal. In this work, we focus on backdoor-based method, which constructs the credit T as a trigger dataset $T = (X_W, Y_W)$ that is only known by the model owner, and train the model such that it can well predict Y_W from X_W [18], [19], [21]:

$$\min_f \mathcal{L}_{\text{CE}}(f(X), Y) + \delta \mathcal{L}_{\text{CE}}(f(X_W), Y_W), \quad (2)$$

where \mathcal{L}_{CE} is the cross-entropy loss. The term $\mathcal{L}_{\text{CE}}(f(X), Y)$ is called the *main task objective* and the term $\mathcal{L}_{\text{CE}}(f(X_W), Y_W)$ is called the *watermark task objective*. $\delta > 0$ controls the trade-off between the two objectives. Since Y_W is secretly known by the model owner, a high classification accuracy on T will justify the ownership of the model.

In addition to the above methods that rely on trigger set, there also exist works choose n-bit string as credit T and directly embed it into the parameters or gradients of machine learning models [15]–[17], [36]. After model training, T will be uploaded to the authority for future ownership verification. Because T is only known to the model owner and the trusted authority, containing the information of T will justify the ownership of the model. The watermark embedding algorithm $\mathcal{E}(D, T)$ should be non-invasive and robust to adversaries.

Watermark verification. Once the ownership of a model is suspected, the model owner may initiate an ownership verification process to justify the true owner of the model. In this process, a trusted third party, such as an government

agency, executes a verification algorithm to determine whether the suspect model satisfies the claimed ownership, denoted as

$$\mathcal{V}(f, T) \rightarrow \{0, 1\}. \quad (3)$$

where f is the suspected model and T is the credit previously uploaded by the true model owner.

The verification algorithms \mathcal{V} are paired with the watermark embedding algorithm \mathcal{E} . For example, when backdoor-based watermark embedding procedure (2) is used, the verification algorithm \mathcal{V} is often realised as checking the prediction accuracy on the trigger set T :

$$\mathcal{V}(f, T) = \begin{cases} 1, & \text{if } \mathbb{E}_{X_W, Y_W \sim T} [\mathbf{1}[f(X_W) = Y_W]] > t \\ 0, & \text{if } \mathbb{E}_{X_W, Y_W \sim T} [\mathbf{1}[f(X_W) = Y_W]] \leq t \end{cases} \quad (4)$$

where $\mathbf{1}$ denotes Indicator function and t is some threshold. This type of method is also called *black-box* verification as it only requires access to the output of the model f . In contrast, algorithms that require full access to the model (e.g., the model's weights) are considered to be *white-box*. Any approach that falls between these two extremes is classified as *grey-box* verification [37]. It is worth noting that white-box verification may pose a significant risk of exposing intellectual property to third parties during the verification process, which can limit its practical applications. In addition, it is essential for a verification algorithm $\mathcal{V}(f, T)$ to be computationally efficient, as the authority requires real-time monitoring of potential intellectual property infringements that may occur online.

D. Watermark Removal Attacks

We consider three representative attacks designed to remove watermarks from the model. Each of these attacks, denoted as $\mathcal{A}(f, D_{\text{aux}})$, takes a victim model f and some auxiliary data D_{aux} as inputs and outputs a new model f^* . A summary of these attacks is provided in Table II.

Knowledge Distillation (KD). This black-box attack [35] steals a model f by training another model f^* to mimic f 's behavior. During the attack, only the output $f(X)$ of the victim model is required. KD works by pairing the logits of f^* and f :

$$\min_{f^*} \lambda \mathcal{L}_{\text{CE}}(f^*(X), Y) + (1 - \lambda) \mathcal{L}_{\text{CE}}(\sigma(f^*(X)/\tau), \sigma(f(X)/\tau)), \quad (5)$$

where the first term is classification loss and the second term is pairing loss, λ controls the balance between two losses. The pairing loss minimize the distance between softened logits of the new model $\sigma(f^*(X)/\tau)$ and the victim model $\sigma(f(X)/\tau)$. Here, σ is the softmax function and $\tau \geq 1$ is distillation temperature whose choice may affect f^* 's performance. Many well-known model stealing attacks are special cases of Formula 5. For example, by setting $\tau = 1$ and

$\lambda = 0$ yields the classic model extraction attack [7], where the adversary lacks ground-truth labels, whereas by setting $\tau = 10$ and $\lambda = 0.5$ we recover the popular distillation attack [35].

Fine-tuning (FT). Unlike KD attack which tries to transfer knowledge to another model in a black-box fashion, this white-box attack [28] removes potential watermark from a specific model by directly modifying its parameters. This is typically done by first fine-tuning the model by a large learning rate η' so as to erase the watermark: $f \leftarrow f - \eta' \nabla_f \mathcal{L}_{CE}(f(X), Y)$, then gradually restoring the model's functionality by smoothly decreasing the learning rate η' . It is shown in [28] that with carefully scheduled the learning rate, most watermarks embedded in a model can be removed without significantly degrading model performance. However, as the attack needs to update model parameters, it necessitates full access to the model, being a white-box attack.

Model pruning (MP). This important type of attack works by directly pruning some neurons in the network, so that the watermark information embedded in the network are destroyed. This is done by first evaluating the importance of each neuron (or weight), then prune the neuron sequentially according to their importance. The pruning process stop terminates when the accuracy of the pruned network has dropped below a pre-defined threshold. A post-processing strategy (e.g. model fine-tuning) is often used to recover the damage due to pruning. Different methods may use different importance metric; for example, fine-pruning (FP) [27] uses the neuron's average activation as the metric, whereas adversarial neuron pruning (ANP) [29] measures the importance of neurons by gradually adding noise to each neuron to see if there is a significant drop in prediction accuracy. Different methods may also focus on pruning neurons in different layers (FP: only focus on the last convolutional layer. ANP: all layers).

Among the above attacks, white-box attacks (FT and MP) are particularly noteworthy because the adversary possesses extensive knowledge about the victim models, making them more capable of removing watermarks. Our primary goal is therefore to develop robust watermark embedding schemes that effectively counter white-box attacks, while also offering protection against black-box attacks.

III. AN INFORMATION-THEORETIC PERSPECTIVE FOR MODEL WATERMARK EMBEDDING

In this section, we analyse existing watermark embedding scheme and corresponding attacks from an information-theoretic perspective, aiming to understand why existing methods are susceptible to watermark erasure attacks. This perspective also serves as a guidance of our own design later.

Watermark embedding as infomax learning. Let f be the DNN model that need to be protected, (X, Y) be the input samples, $T = (X_W, Y_W)$ be a trigger set picked by model owner, S be some internal representation in f computed for X , i.e., $S = s(X)$, and the decision making process of the DNN satisfies the following Markov chain:

$$X \rightarrow S \rightarrow \hat{Y}, \quad (6)$$



(a) Normal img (b) Trigger, ours (c) Trigger, ours (d) Trigger, [18]

Fig. 1: Examples of trigger set for watermark embedding. (a), (b), and (c) are the trigger set used in this work based on in-distribution images. Specifically, (b) rotates the image in (a) and (c) changes the color in (a). (d) presents the trigger set that use out-of-distribution images follows [18].

where \hat{Y} be the predicted label. The same Markov chain holds for samples X_W, Y_W in the trigger set T . A well-trained network will yield S being a near-sufficient statistics for Y , i.e., $I(S; Y) \approx I(X; Y)$, where $I(\cdot; \cdot)$ denote the mutual information between two random variables.

For black-box watermarking schemes, which embed watermarks as Equation (2), its watermark embedding process can be shown to be equivalent to maximizing the mutual information between the learned representation $s(X_W)$ and Y_W :

$$\max_s I(s(X); Y) + \delta I(s(X_W); Y_W). \quad (7)$$

which is a direct consequence of Proposition 2 in [38]. In this regard, the watermark verification process (4) can be seen as measuring whether $I(s(X_W); Y_W)$ is high enough for a suspicious model, where only high $I(s(X_W); Y_W)$ will indicate the ownership:

$$\mathcal{V}(f, T) = \begin{cases} 1, & \text{if } I(s(X_W); Y_W) > t' \\ 0, & \text{if } I(s(X_W); Y_W) \leq t', \end{cases} \quad (8)$$

where t' is some threshold.

Watermark removal as information-theoretic game. Therefore to erase the watermark embedded in a model, an adversary needs to reduce $I(s(X_W); Y_W)$ as much as possible while maintaining a reasonably high $I(s(X); Y)$. This can be mathematically formulated by the following objective:

$$\min_s I(s(X_W); Y_W) \text{ s.t. } I(s(X); Y) \geq (1 - \epsilon)I(X; Y) \quad (9)$$

where $\epsilon \approx 0$ is a small positive value. A strong attack will find a good function $s(\cdot)$ whose corresponding ϵ is small. Below, we show that an adversary can easily find such s if there is little overlap between $p(X)$ and $p(X_W)$, where $p(X)$ denotes the distribution of X .

A. Pitfalls of Out-of-distribution Trigger-set

Based on the information-theoretic viewpoint above, we now analyse why many existing methods for model watermarking must fail in the presence of watermark erasure attacks. Specifically, these existing schemes largely make use of *out-of-distribution* trigger set $T = \{X_W, Y_W\}$ where $p(X_W)$ hardly overlap with $p(X)$; see Fig. 1. We argue that these outlier-based methods are by construction problematic, as an adversary can easily reduce the value of $I(S_W; Y_W)$ without affecting the value of $I(S; Y)$ in Equation (7). See Theorem 1 below:

Theorem 1 (Limitations of out-of-distribution schemes). *Consider random variables $X, X_W \in \mathbb{R}^D$ and $Y, Y_W \in \mathbb{R}$. As $KL[p(X)||p(X_W)] \rightarrow \infty$, there exist infinitely many functions g^* such that $g^* = \arg \max_g I(g(X); Y)$ and $I(g^*(X_W); Y_W) = 0$.*

Proof. As $KL[p(X)||p(X_W)] \rightarrow \infty$, there exists a classifier $c : \mathbb{R}^D \rightarrow \{0, 1\}$ to perfectly distinguish samples $x \sim p(X)$ and $x \sim p(X_W)$. Without loss of generality we assume that the output for this classifier is 1 for $x \sim p(X)$ and 0 for $x \sim p(X_W)$ i.e.

$$\begin{cases} c(x) = 1, & \forall x \sim p(X) \\ c(x) = 0, & \forall x \sim p(X_W). \end{cases}$$

Now consider g constructed as follows:

$$g(X) = (\gamma g^*(X)) \circ c(X),$$

where $\gamma \neq 0$ is any non-zero real value. It is clear that g satisfies:

$$\begin{cases} g(x) = \gamma g^*(x), & \forall x \sim p(X) \\ g(x) = 0, & \forall x \sim p(X_W). \end{cases}$$

It immediately follows that $I(g(X); Y) = I(\gamma g^*(X); Y) = I(g^*(X); Y)$ and $I(g(X_W); Y_W) = 0$. Since g^* maximises $I(g(X); Y)$, this completes the proof. \square

In other words, so long as there is only little overlap between $p(X_W)$ and $p(X)$, the internal representation S_W of the model can be made as uninformative about Y_W as possible while keeping highly informative about Y . This essentially means that the attack goal Equation (9) has been achieved. In fact, from the proof of Theorem 1, one can also see that the degree that an adversary can reduce $I(s(X_W); Y_W)$ depends on the degree that $p(X)$ and $p(X_W)$ overlap. Therefore to resist watermark erasure attacks, a certain level of overlapping between $p(X)$ and $p(X_W)$ must exist.

We conduct a simple experiment to support our theory. In experiments, we train the model and embed watermark with Adi’s method [18], where the trigger sample X_W is out-of-distribution. Then, we extract activations of the convolutional layers in the third block of ResNet-18 for the inputs, including training samples, augmented training samples, and the out-of-distribution samples. Then we normalize these activations to $[0, 1]$ and plot their heatmaps, see Fig. 2. As we can see, neurons activated by out-of-distribution samples differ significantly from those activated by in-distribution samples, making it easy to distinguish trigger samples from normal samples in the latent space. This differentiation facilitates the subsequent networks to remove watermarks without impairing model performance.

The above analysis also implies that recent watermarking schemes based on out-of-distribution trigger set may not truly protect the ownership of models. For example, the works [21], [35] encourage the overlap between the representation computed for X and the internal representation computed for X_W , in hope that such overlapping in representational space can avoid the adversary from easily removing watermarks. If we treat these internal representations as the inputs X and X_W for the downstream network, then these methods can be seen as seeking $KL[p(X)||p(X_W)]$ to be small at *representation*

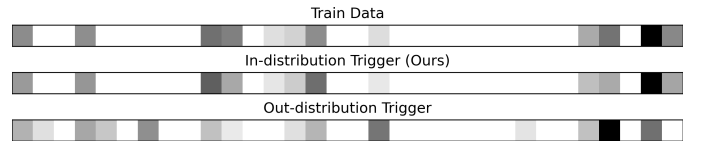


Fig. 2: Heatmap of inner activation in deep neural networks for in-distribution and out-of-distribution trigger sets. The darker colors indicates larger activations.

level, so that any downstream network will not suffer from the previously mentioned issue. However, there is no guarantee on the upstream network used to compute these representations, so the whole network is still vulnerable to attacks. In fact, it has been recently shown that defenses like [21] is not so secure as originally claimed [36].

B. On Logits as Watermark Information Carrier

The above analysis also implies that the predicted label alone may not be sufficient to carry the information about watermark. To see this, consider the case where there is a significant overlap between $p(X)$ and $p(X_W)$ — a necessary condition for defending against watermark removal attack. In such case, there exist lots of samples in $x \sim p(X)$ and $x_W \sim p(X_W)$ whose semantic labels are the same. For these samples, the model prediction would be exactly the same, leaving there no room to embed any further information. In other words, we need richer information carrier to carry the watermark information.

Our proposal here is to make use of the full logits $f_1(X_W), \dots, f_K(X_W)$ rather than solely using the model prediction (i.e., the index of the maximal logit) in watermark verification, which can in essence carry more information about the watermark. This concept is closely related to Membership Inference Attacks (MIA) [39], which reveal that logits contain rich information about whether a sample belongs to a specific dataset. Here, we also utilize this phenomenon, but in a way that we use it to show the affinity of the model to a secret dataset.

The question remained is how to embed watermark information in the logits and how to extract watermark information from them. To answer this question, we first introduce the concept of *redundant logits*, which is defined as below:

Definition 1 (Redundant logits). *Define \mathcal{I}_{top-k} to be the indices of the top k largest elements of the logits: $\{f_1(x), \dots, f_K(x)\}$. A logit $f_j(x)$ is said to be redundant if $j \notin \mathcal{I}_{top-k}$. Here $k \ll K$.*

An interesting property of redundant logits is that most of the information about the label Y is not in the redundant logits, namely:

$$I(f_{\mathcal{I}_{top-k}}(X); Y) \approx I(f(X); Y), \quad (10)$$

where $f_{\mathcal{I}_{top-k}}(X)$ is a function extract the top- k logits from the original logits $f(X)$. The rationale behind (10) is the ground truth label is often among the top- k prediction of the model, so that the values of non-top- k logits are indeed irrelevant for model prediction. In fact, if we slightly manipulate the values

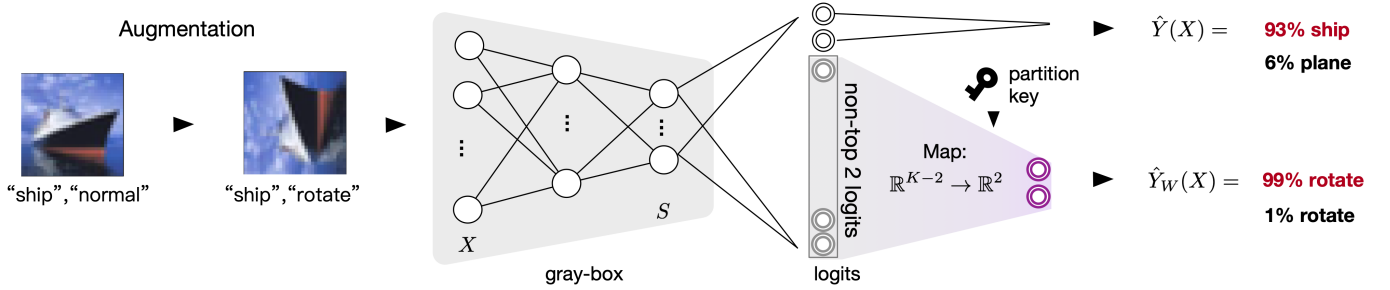


Fig. 3: An overview of the proposed IWE method. When computing the logits of the watermark task (WT), i.e., the purple double circles in the figure, we map the redundant logits (e.g., the non-top-2 logits of the main task, represented by the grey double circles) to WT logits. This mapping process is controlled by a partition key only known to the model owner. During ownership verification, only the logits, the partition key, the trigger set and the computation graph of the model will be exposed.

of the non-top- k logits, most predictions \hat{Y} will still remain correct². This is also why we call these logits redundant logits.

The existence of redundant logits create us additional space for embedding watermark information without affecting the original prediction. In the next section, we will show how to use these redundant logits to embed watermarks in practice, so that the potential conflict between the main task and the watermark task is minimised.

A notable risk of using (redundant) logits as information carrier is that it may suffer from potential *logit lair* attack where the adversary returns fake logits during watermark verification. We will analyze the impact of logit lair attack in Section VI.

IV. IN-DISTRIBUTION WATERMARK EMBEDDING

In this section, we propose a new model watermarking scheme, named *In-distribution Watermark Embedding (IWE)*, aiming to overcome the aforementioned fundamental limitation of existing methods. Our method is designed to achieve the following two desiderata in one framework:

- *Resist white-box attacks.* Our method is designed to be effective even when the model parameters are completely revealed to the adversaries;
- *Support gray-box verification.* Our method only needs to inspect the logits during ownership verification, though we reserve the right to open the box in case of logit liar attack.

Below, we show how to achieve these goals by a new *trigger set construction* scheme and a novel *redundant logits reusing* scheme. An overview of our method is in Fig. 3.

A. Design of In-distribution Trigger-set

From the above analysis, it is clear that there must be a certain overlap between the trigger set and normal samples. On the other hand, there must still be some difference between trigger set and normal samples, otherwise any model that attains high main task performance will automatically pass ownership verification. Therefore the key is a proper level of overlapping.

²This can also be justified by considering the detailed contribution of each logit in the cross-entropy loss: $\mathcal{L}_{\text{CE}}(f(x), y) = -\sum_k y_k \log f_k(x) = -y_{k^*} \log f_{k^*}(x)$, where only maximal element in the K logits will participate in the calculation of the CE loss if y is a one-hot vector: $y \in \{0, 1\}^K$: $\sum_{k \neq k^*} y_k = 0$, $y_{k^*} = 1$. Only the value of the top-1 logit affects the loss.

To this end, we design the trigger set as a dataset with a moderate overlap level using *in-distribution* samples. More specifically, we construct the trigger set T as the union of normal samples and their augmented versions:

$$T = (X_W, Y_W) = \{(x, 0)\} \cup \{(x_{\text{aug}}, 1)\}_{x \in D'}, \quad (11)$$

where x_{aug} is some augmented version of sample x , and D' is a subset of training dataset D , $D' \subset D$. Therefore the trigger set is comprised of a subset of normal samples (with assigned labels $y_w = 0$) and the augmented samples (with assigned labels $y_w = 1$). While any data augmentation techniques can be used to generate x_{aug} in principle, we focus on the following two operations due to their simplicity:

- *Rotation.* This corresponds to applying a rotation matrix \mathbf{R} to the input x :

$$x_{\text{aug}} = \mathbf{R}x, \quad \mathbf{R} = \begin{bmatrix} \cos \theta & -\sin \theta \\ \sin \theta & \cos \theta \end{bmatrix}, \quad (12)$$

where θ is the rotation angle.

- *Color adjustment.* This corresponds to changing the brightness, contrast and saturation level of the image [40]:

$$x_{\text{aug}} = \mathcal{C}(x; \gamma_1, \gamma_2, \gamma_3), \quad (13)$$

where \mathcal{C} is a function to modify the brightness, the contrast and the saturation level of an image and $\gamma_1, \gamma_2, \gamma_3$ are the corresponding controlling hyperparameters.

Under this setup, the watermark embedding task is now formulated as a binary classification task where we predict whether a sample X_W is augmented or not

$$\mathcal{L}_{\text{CE}}(f(X_W), Y_W) = \mathbb{E}[-\log p_f(Y_W | X_W)], \quad (14)$$

where $p_f(Y_W | X_W)$ is the class probability parameterized by the model f . The only question remains is how to compute the binary class probability $p_f(Y_W | X_W)$ from the network f , which is originally designed to compute the class probability $p_f(Y | X_W)$ for K -classes rather than two classes. We explain below how to compute $p_f(Y_W | X_W)$ without introducing additional network modules.

Algorithm 1: Watermark Embedding $\mathcal{E}(D, T, \mathcal{K})$

Input: Training set $D = \{X, Y\}$, triggers set $T = \{X_W, Y_W\}$, partition key \mathcal{K}
Output: Watermarked model f
Hyperparams: δ, η, N

- 1 Initialize f ;
- 2 **while** epoch : $1 \rightarrow N$ **do**
- 3 **for** each batch **do**
 - 4 // 1. get main task loss
 - 4 Sample batch $\{x^{(i)}, y^{(i)}\}_{i=1}^B$;
 - 5 Compute $\ell_{\text{main}} = \frac{1}{B} \sum_i \mathcal{L}_{\text{CE}}(f(x^{(i)}), y^{(i)})$;
 - 4 // 2. get watermark task loss
 - 6 Sample batch $\{x_W^{(i)}, y_W^{(i)}\}_{i=1}^B$;
 - 7 Compute $\ell_{\text{wm}} = \frac{1}{B} \sum_i \mathcal{L}_{\text{CE}}(f(x_W^{(i)}), y_W^{(i)}; \mathcal{K})$;
 - 8 $f \leftarrow f - \eta \nabla_f (\ell_{\text{main}} + \delta \ell_{\text{wm}})$;
- 9 **return** f

B. Redundant Logit Reusing

We explain here how to compute $p_f(Y_W | X_W)$ from the original class probabilities $p_f(Y = k | X_W) \propto e^{f_k(X_W)}$ without introducing any additional modules. In this work, we compute $p_f(Y_W | X_W)$ by reusing the logits $f_k(X_W)$ in the original class probabilities:

$$\begin{aligned} p_f(Y_W = 1 | X_W) &\propto e^{\frac{1}{|\mathcal{K}|} \sum_{k \in \mathcal{K} \setminus \mathcal{I}_{\text{top-}k}} f_k(X_W)} \\ p_f(Y_W = 0 | X_W) &\propto e^{\frac{1}{|\bar{\mathcal{K}}|} \sum_{k \in \bar{\mathcal{K}} \setminus \mathcal{I}_{\text{top-}k}} f_k(X_W)}, \end{aligned} \quad (15)$$

where $\mathcal{I}_{\text{top-}k}$ is the indices of the largest k elements in the array $\{f_1(X_W), \dots, f_K(X_W)\}$ (i.e., the indices of non-redundant logits) and \mathcal{K} is the so-called *partition key* defined as below. $\bar{\mathcal{K}}$ is the complement of \mathcal{K} w.r.t the set $\mathcal{I} = \{1, \dots, K\}$.

Definition 2 (Partition key). *A partition key $\mathcal{K} \subset \mathcal{I}$ is a subset of the set of indices $\mathcal{I} = \{1, \dots, K\}$ whose size $|\mathcal{K}| = \lceil K/2 \rceil$.*

In other words, we calculate the new class probabilities $p_f(Y_W | X_W)$ by first excluding the top- k logits, then computing the probabilities for class $Y_W = 0$ and class $Y_W = 1$ from the remaining logits according to their assigned partitions. This way, we turn the logits in a K -way classification problem into the logits in a binary classification problem, without introducing any additional component to the model.

The rationale behind the above method for computing $p_f(Y_W | X_W)$ is the information-theoretic analysis in III-B, which reveals that non-top- k logits are indeed irreverent for predicting Y and can therefore be used to carry watermark information. Importantly, due to the redundancy of these non-top- k logits, the information they carry will not obscure the primary information in the top- k logits, thereby will not impact the main task performance.

Once the training of the model is done, the partition key \mathcal{K} is no more used in the network and will be kept secret by the model owner. During verification, the model ownership needs to present both T and \mathcal{K} to the authority to pass ownership verification. In this sense, the partition key \mathcal{K} can be seen as part of the trigger set T .

Algorithm 2: Watermark verification $\mathcal{V}(f, T, \mathcal{K})$

Input: Suspicious model f , trigger set T and partition key \mathcal{K} , population of clean models $\mathcal{F}_{\text{clean}}$,
Output: Ownership testing outcome
Hyperparams: significance level α

- 1 $\mathcal{G} = \emptyset$;
- 2 **for** $f' \in \mathcal{F}_{\text{clean}}$ **do**
 - 3 // 1. threshold computation
 - 3 $\mathcal{G} \leftarrow \mathcal{G} \cup \{\text{ACC}_W(f')\}$;
- 4 $t \leftarrow (1 - \alpha)\%$ quantile of \mathcal{G} ;
- 4 // 2. threshold comparison
- 5 **if** $\text{ACC}_W(f) < t$ **then**
- 6 Accept H_0 in (16) and set $Y = 0$;
- 7 **else**
- 8 Reject H_0 and set $Y = 1$.
- 9 **return** Y

The whole watermark embedding procedure for the proposed IWE method is summarized in Algorithm 1.

V. WATERMARK VERIFICATION

A crucial question remained is how to verify the watermark for a suspicious model f . Statistical hypothesis testing offers a principled way for verifying the existence of the watermark in a model. Formally, let $\mathcal{F}_{\text{clean}}$ be the population of clean models (i.e., models on the same task but without watermark T), we test the null hypothesis H_0 against the alternative H_1 below:

$$\begin{cases} H_0 : f \in \mathcal{F}_{\text{clean}} \\ H_1 : f \notin \mathcal{F}_{\text{clean}}, \end{cases} \quad (16)$$

where the test statistics is defined as the accuracy on the trigger set, i.e.,

$$\text{ACC}_W(f) = \mathbb{E}_{X_W, Y_W \sim T} [\mathbf{1}[f(X_W) = Y_W]], \quad (17)$$

where $\mathbf{1}$ denotes the indicator function and \mathcal{K} is the aforementioned partition key. Here $f(X_W)$ is the network's prediction: $f(X_W) = \arg \max_{Y_W} p_f(Y_W | X_w)$ with $p_f(Y_W | X_w)$ computed as (15).

We reject H_0 if the corresponding P-value of the test statistics $\text{ACC}_W(f)$ is smaller than a pre-defined significance level α (e.g., 5%). In other words, if we find that $\text{ACC}_W(f)$ is significantly high compared to the majority (e.g., 95%) of the clean models, then f is likely to be a watermarked model (and hence indicates model ownership). The whole process of this hypothesis testing-based watermark verification procedure is summarized in Algorithm 2.

We highlight that the above hypothesis testing-based watermark verification method is very generic and can be applied to any backdoor-based model watermarking schemes, e.g., [17], [18], [20], [21]. Such universal applicability also provides us with an unified way to systematically compare among different watermark embedding schemes with different setups. For example, by comparing the true positive rate (TPR) i.e., the probability that we correctly identify the watermark in the

above hypothesis testing-based decision making process, we are able to compare the true reliability of various watermark schemes even if their design of trigger set are largely different (e.g., having different number of classes in their trigger sets).

VI. SECURITY ANALYSIS

In this section, we provide security analysis of our IWE method in the presence of two types of attacks. The first type of attack aims at attacking the trigger set, where the adversary tries to pass verification by either guessing the trigger set directly or forging a fake trigger set. The second type of attack focuses on manipulating the values of logits, which can be seen as adaptive attacks that make use of the logits exposed in our method to pass ownership verification.

A. Attacking the Trigger Set

Guessing the trigger-set. The first threat we consider is directly guessing the trigger set T to pass ownership verification. Since T serves as the credit of model ownership, a direct breach of T will pose serious security threat. We note that directly guessing T is highly difficult in our IWE method. Specifically,

- *Difficulties in forging trigger images.* The construction of a trigger set involves the choice of base images and applying the augmentation operations. For the choice of base images, we first choose K' classes out of the K classes ($K' \ll K$), then randomly draw samples from these K' classes. Therefore the probability of successfully guessing the trigger set is at most $P_1 = \frac{K'}{K} \times \frac{1}{N_{\text{aug}}}$, where N_{aug} is the number of possible augmentation choices (there are numerous augmentation methods available in image processing. This includes adjusting the hyperparameters used in augmentation operations, e.g., rotation angles, brightness and saturation);
- *Difficulties in forging partition key.* There are multitude choice for the partition key \mathcal{K} , rendering it difficult to forge. According to Definition 2, the total number of possible choice of \mathcal{K} is $\binom{K}{K/2}$. The probability of successfully guessing a particular \mathcal{K} is therefore $P_2 = 1/\binom{K}{K/2}$, which is $1/252$ for $K = 10$ and is no more than $1/10^{28}$ for $K = 100$.

Jointly considering these two difficulties, the probability P_{success} of successfully forging both factors: $P_{\text{success}} = P_1 \times P_2$ is indeed small. Therefore an adversary is unlikely to forge the ownership proof within a few attempts.

Forging a fake trigger set. The second security threat we consider is directly forging a trigger set $T' \neq T$ that can pass verification. Specifically, let f be the victim model and $T' = \{X_W^{(i)}, Y_W^{(i)}\}_{i=1}^n$ be the ‘fake’ trigger set constructed by the adversary. Consider constructing T' by setting $Y_W^{(i)}$ as

$$Y_W^{(i)} = f(X_W^{(i)}) \quad (18)$$

for arbitrarily chosen $X_W^{(i)}$. In this scheme, since T' and f perfectly match with each other, the adversary is able to claim the ownership of f by presenting T' to the authority even without modifying f , posing a serious security threat.

We note that this threat of trigger set forgery is not unique for our method: it exists in all trigger set-based watermark embedding schemes, e.g., [18], [20], [21], so long as one

verifies the model ownership by solely comparing the output of the model and the presented trigger set, which can be forged.

Our solution to defend against trigger set forgery attack is to ask the model owner to prove the credence of the trigger set T . This can be done by showing that there exists another ‘shadow model’ $f' \neq f$ belonging to the same model owner that also *match well with T but have equally-high utility*. The rationale behind this method of ‘double model verification’ is that if one truly owns the model f , then he must be able to train multiple highly-functioning models that can match well with T but are vastly different in the parameter space (e.g., by using different initialization in training). This is however difficult for a model stealer who does not know f' in advance. The adversary may of course try to construct a fake f' by e.g., fine-tuning f with the fake T' with a small learning rate. However, the fine-tuned f' may still remain close to f in the parameter space, being easy to detect that it originates from f . In practice, we can simply compare the L_2 norm between f and f' presented by each party, and the party whose models f, f' have a larger norm is more likely to have the true ownership of the model.

B. Logit Lair Attack

Adding noises to logits. In this section, we further discuss the threat of possible adaptive adversary. An adaptive adversary has full knowledge of the technical details of our defense, and can make use of such knowledge to design attack accordingly. One adaptive attack is to inject some random noises to the output of the logits, similar to the attacks in [22], [31]:

$$f_i(x) \leftarrow f_i(x) + \xi_i, \quad (19)$$

where the noise $\xi_i \sim p(\xi)$ is drawn from some distribution $p(\xi)$ with finite mean μ and finite variance σ^2 . This attack exploits the nature of our method that we rely on the values of the logits in ownership verification.

We argue that our method is immune to this kind of attack by nature. This is because the added noises will automatically cancel out during the computation of class probabilities in Equation (15). To see this, recall that when computing Equation (15), we sum and average the logits $\{f_1(x), \dots, f_K(x)\}$ according to their belonging groups. As a result, the injected noises ξ_i will also be averaged. The variance of these averaged noises will be $\mathbb{V}\left[\frac{1}{K/2} \sum_i^{K/2} \xi_i\right] = \frac{2}{K} \mathbb{V}[\xi_i] = \frac{2}{K} \sigma^2$, which fades out as $K \rightarrow \infty$. This means that with moderately large K , the effect of the added noises will be eliminated. On the other hand, the mean of the added noises $\mathbb{E}\left[\frac{1}{K/2} \sum_i^{K/2} \xi_i\right] = \mathbb{E}[\xi_i] = \mu$ will be canceled out when computing the softmax probabilities in Equation (15). Putting all together, our method is safe under this attack with reasonably large K (e.g., $K \geq 10$). We highlight that the above analysis has not assume the distribution family of $p(\xi)$ holds for all distribution family that ξ_i samples from.

In addition, our method is by design robust to evasion attacks [22], [31], a representative adaptive attack that works by detecting and evading an ongoing ownership verification request. This types of attack typically works by anomaly detection, yet the trigger set samples in our method highly resemble normal samples, rendering anomaly detection difficult and ownership verification requests undetectable.

Replacing redundant logits. Since our watermark scheme rely on logits to verify watermarks, a natural attack is to simply replacing some of the logits by arbitrary values during ownership verification. For example, the adversary can use the output logits in another network to replace the redundant logits in the original network. Since only the redundant logits are replaced, this will not impair the utility of the original network. We note that such logit replacement attack is unable to defend in black-box settings, where the adversary only expose the logits during ownership verification (e.g., a cloud-based API). We thereby require one to expose the full computational graph of the model during model ownership verification to avoid an adversary from providing fake logits. This requirement ensembles those of white-box watermarking schemes e.g., [17], [41], however the verification process of our method is still much light-weighted compare to white-box watermark verification methods as we only need to check the output of the model and the computational graph rather than the full parameters of the model. This will be further ascertained by our experiments, where we compare the execution time of our method with both black-box and white-box approaches.

VII. EXPERIMENT

In this section, we conduct extensive experiment to verify the effectiveness of proposed method. We first introduce the setup of the experiments, including datasets, neural networks, attacks, and evaluation metrics. We then assess the proposed IWE to show fidelity and robustness. In particular, we take both white-box and black-box attacks in to considerations.

A. Setup

Datasets. We use three real-world datasets in experiments: CIFAR-10, CIFAR-100 and Caltech-101. The first two datasets are chosen so as to follow existing works on watermark embedding [18], [28], [35]. We additionally incorporated the Caltech101 dataset [42] as the resolution of the image in this dataset resembles that of ImageNet, making it a choice highly closer to realistic settings.

- *CIFAR-10.* It consists of 32×32 color images of real-world objects. These objects are divided into 10 classes, with 5000 instances per each class in the training set and approximately 1000 instances per each class in the test set.
- *CIFAR-100.* It contains similar images as in CIFAR-10, but the classes are further divided into 100 more fine-grained categories, being more challenging than CIFAR-10.
- *Caltech101.* It consists of natural images of 101 categories, with 40 to 800 color images per each category. Each image is resized to 224×224 pixels.

Neural networks architecture and training. In this work, we consider two commonly-used deep neural network architectures in computer vision:

- *ResNet-18.* This architecture is used for CIFAR-10 and CIFAR-100. We use stochastic gradient descent (SGD) with momentum to optimize the network, where the momentum value is set to be 0.9. A small weight decay (5×10^{-4}) is further used to avoid overfitting. We train the model for 100

epochs, where we set the learning rate to be 10^{-2} , 10^{-3} , and 10^{-4} for epochs 1 to 50, 51 to 75, and 75 to 100 respectively.

- *ResNet-34.* This architecture is used for Caltech101. The model is first pre-trained on the ImageNet dataset, then fine-tuned on Caltech101 for 50 epochs. The pre-trained model is available at the official website of PyTorch. During fine-tuning, we use SGD as the optimizer, and the learning rate is set to be 5×10^{-3} , 5×10^{-4} and 5×10^{-5} for epochs 1 to 20, 21 to 35, and 36 to 50, respectively.

The two network architecture choices above cover both the cases of training from scratch and pre-trained model.

IWE implementation details. The details of the configuration of trigger set construction and watermark embedding of IWE are as follows:

- *Trigger set construction.* Recall that to construct the trigger set, we first choose a subset of data from the normal training dataset, then apply argumentation operations on these data. For subset selection, we opt for half of the class 8 and 9 images for CIFAR-10, half of the class 0, 1, and 2 images for CIFAR-100, and half of the class 10 images for Caltech101. This selection is completely random. For argumentation operations, we use $\theta = \pi/2$ for rotation operation and we apply the ‘‘ColorJitter’’ operation in PyTorch with parameters $\lambda_1 = 0.8$, $\lambda_2 = 0.8$, and $\lambda_3 = 0.8$ for color adjustment. An example of the their trigger set image is presented in Fig. 1.
- *Watermark embedding.* We follow Algorithm 1 precisely to embed watermarks. After that, we use *fine-tuning post-processing techniques* to repair the utility damage caused by watermark embedding. In experiments, we find that an additional fine-tuning step can help further improve the performance of our method slightly. More specifically, after learning the watermarked model, we use a learning rate η' that is much smaller than standard learning rate η to fine-tune the model on the main task by a small number of training steps. As studied in previous studies [18], [28], a small learning rate is typically not enough to erase watermarks, yet it is helpful to repair the potential damage caused by watermark embedding. In particular, we set the learning rate in this fine-tuning stage to $\eta' = 10^{-5}$ and fine-tune the model for only one epoch. We find that this setup is robust across different dataset (in fact, any choice $\eta' \in [10^{-4}, 10^{-7}]$ also works quite well).

A summary of the IWE experiment settings is given in Table III.

Attack details. We consider the four adversaries mentioned in section II-D: KD, FT, FP, and ANP. These attacks cover the cases of both white-box (FT, FP, ANP) and black-box (KD) attacks. Following existing works [28], [35], [43]–[45], we assume that all adversaries has 20% of the training data. The detailed setups of the adversaries are as follows:

- *Knowledge distillation (KD) adversary.* For this adversary, we use soft label distillation, where the hyper-parameters λ and τ in Equation (5) is set to be $\lambda = 1$ and $\tau = 10$. This setup is the same as the well-known distillation attack [35]. In addition, we also assume that the adversary in this attack can obtain pre-trained models, such as ResNet-34 pre-trained on ImageNet when attacking Caltech101. This

TABLE III: IWE experiment settings. Here δ is the trade-off factor between the main task and the watermark task in Equation (2), k is the number of maximal logits we exclude in Equation (15), η' is the learning rate used in post-processing fine-tuning.

Dataset	Network	Pretrained	Train	Test	δ	m	η'	Epoch	WT task	Adversary's data
CIFAR-10	ResNet-18	False	50000	10000	0.01	3	1e-5	100	Rotation	10000
CIFAR-100	ResNet-18	False	50000	10000	0.03	3	1e-5	100	Rotation	10000
Caltech-100	ResNet-34	True	6941	1736	0.02	2	1e-5	50	ColorJitter	1388

TABLE IV: Fidelity Comparison. We report main task ACC and watermark task ACC_W across different models. Each result is the mean of 20 independent runs. Clean models mean no watermark embedded. Bold text indicates the high-fidelity model.

Dataset	Clean models		IWE (Ours)		EWE [21]		Adi [18]		Zhang [20]		Bansal [17]	
	ACC	ACC_W	ACC	ACC_W	ACC	ACC_W	ACC	ACC_W	ACC	ACC_W	ACC	ACC_W
CIFAR-10	94.6%	47.1%	94.6%	96.9%	91.5%	99.8%	94.1%	100.0%	94.2%	100.0%	92.4%	100%
CIFAR-100	75.6%	48.8%	75.6%	91.9%	69.2%	77.4%	74.6%	100.0%	74.6%	100.0%	72.2%	100%
Caltech-100	96.2%	49.3%	96.1%	99.0%	82.0%	31.9%	96.3%	100.0%	96.2%	100.0%	95.4%	100%

is a reasonable assumption since pre-trained model is often publicly available.

- *Fine-tuning (FT) adversary*. For this attack, we follow the implementation in REFIT [28], one of the most powerful instance in this category. Specifically, we set the initial learning rating to be $0.05 \times (\text{length of batch size} // 64)$, then multiply it by 0.9 every epoch during the attack. A total number 60 epochs is used for this attack ³.
- *Fine-pruning (FP) adversary*. Recall that fine-pruning [27] is a two-stages attack. In the first stage, we prune 0 – 99% (default setting is 99%) of less important filters of the *last convolutional layer* as done in the author’s work ⁴. In the second stage, we fine-tune the model for 50 epochs with a learning rate of 0.001, following the setup in [46] (we use this open-source implementation as the author has not provided the implementation for this stage).
- *Adversarial neuron pruning (ANP) adversary*. For this attack, we follow the author’s official implementation ⁵ and set the maximal pruning percentage to be 90% (default setting is 20%). Note that ANP needs to modify the architecture of a model, where it replaces all batch-norm layer with another layer called noised batch-norm layer. This makes ANP inapplicable to the case with pretrained model, e.g., Caltech101 settings, so we do not apply ANP on this dataset.

Baseline implementation details. We subject our IWE technique to a rigorous comparison with both black-box watermark embedding methods and white-box alternatives.

Here is a breakdown of our implementation process:

- *Adi [18] and Zhang [20]*: Implemented using their provided PyTorch code with default settings.
- *Bansal [17]*: Both Bansal^{bb} (the black-box version of the method) and Bansal^{wb} (the white-box version of the method) are implemented, utilizing their provided PyTorch code.
- *EWE [21]*: We adapt their TensorFlow code to PyTorch and validate that the results of our implementation are consistent with the original paper. We then extend their method to Caltech101 according to CIFAR100 settings.

³<https://github.com/sunblaze-ucb/REFIT>

⁴<https://github.com/kangliuon/Fine-pruning-defense>

⁵https://github.com/csdongxian/ANP_backdoor

All implementations including our proposed IWE method will be made accessible on public repository upon acceptance.

B. Metrics

We evaluate the performance of different watermark embedding methods from two angles, namely (a) fidelity and (b) robustness against watermark erasure attacks.

Fidelity. The first criterion for evaluation is the accuracy of a watermarked model on the main task, which is defined as:

$$ACC(f) = \mathbb{E}[1[f(X) = Y]], \quad (20)$$

where the expectation is taken over the test set. Ideally, the ACC of a watermarked model should be close to that of a clean model as much as possible.

Robustness against attacks. The second evaluation criterion is the robustness of a given watermark embedding scheme against watermark removal attacks. This robustness can in theory be assessed by comparing the ROC curves of different watermark schemes, which plot the true positive rates (TPR, defined as the likelihood of correctly detecting a watermark in a stolen model) against the false positive rates (FPR, defined as the likelihood of mistakenly identifying a clean model as watermarked) under a specific attack. Here, instead of comparing the ROC curves of different schemes, we focus on comparing the TPR at a fixed FPR of 5%, as cases with high FPRs are less relevant to our interests. A higher TPR at this level of FPR will indicate a more robust defense against attacks.

Specifically, consider n watermarked models f_1, \dots, f_n which are trained using the same trigger set T , partition key \mathcal{K} (if applicable) but different random seeds. We calculate TPR at $FPR = 5\%$ (denoted as $TPR@5\%FPR$) as follows:

$$TPR@5\%FPR = \frac{1}{n} \sum_{i=0}^n \mathcal{V}(f_i^*, T, \mathcal{K}), \quad (21)$$

where f_i^* represents the stolen version of f_i and \mathcal{V} is the watermark verification process outlined in Section V; see Algorithm 2 for its details. The significance level α in Algorithm 2 is set to be 5%, which corresponds to a FPR of 5% in decision making. Similar metric has also been adopted

TABLE V: Comparing the watermark robustness of IWE with the baseline methods. ΔACC indicates the accuracy drop when under attack (as compared to the case before attack). $\text{TPR}@5\%\text{FPR}$ represents the probability of correctly identifying watermarked models when the false alarm rate equals to 5%. Either large ΔACC or high TPR indicates an unsuccessful attack. The values of ACC_W are only for reference and are not directly comparable as the numbers of classes in the watermark task are different (IWE: binary classification; Baseline: K -way classification where K is the number of classes in the main task).

Dataset	Method	FT [28]			FP [27]			ANP [29]			KD [35]		
		ΔACC	ACC_W	$\text{TPR}@5\%\text{FPR}$	ΔACC	ACC_W	$\text{TPR}@5\%\text{FPR}$	ΔACC	ACC_W	$\text{TPR}@5\%\text{FPR}$	ΔACC	ACC_W	$\text{TPR}@5\%\text{FPR}$
CIFAR-10	IWE (ours)	3.4%↓	63.8%	100%	0.1%↓	91.7%	100%	23.3%↓	85.3%	100%	5.4%↓	89.9%	100%
	EWE [21]	4.2%↑	9.2%	60%	4.1%↑	40.7%	95%	23.7%↓	41.6%	100%	2.7%↓	11.7%	80%
	Bansal ^{wb} [17]	3.0%↓	45.7%	100%	1.2%↓	48.7%	100%	69.6%↓	85.5%	100%	3.0%↓	15.2%	60%
	Bansal ^{bb} [17]	3.0%↓	1.6%	45%	1.2%↓	90%	90%	69.6%↓	88.5%	95%	3.0%↓	3.0%	45%
	Adi [18]	3.8%↓	15.7%	20%	0.4%↓	98.7%	100%	27.0%↓	22.4%	95%	2.9%↓	15.4%	20%
	Zhang [20]	4.0%↓	0.5%	5%	0.4%↓	94.2%	100%	38.2%↓	0.0%	0%	3.0%↓	0.7%	10%
CIFAR-100	IWE (ours)	6.8%↓	64.5%	100%	0.3%↓	84.3%	100%	60.7%↓	67.8%	100%	7.9%↓	70.6%	100%
	EWE [21]	4.7%↓	6.2%	100%	0.0%↓	60.1%	100%	51.8%↓	15.5%	50%	6.5%↓	26.0%	100%
	Bansal ^{wb} [17]	6.4%↓	46.9%	100%	1.3%↓	65.6%	100%	44.8%↓	85.4%	100%	8.4%↓	1.7%	65%
	Bansal ^{bb} [17]	6.4%↓	0.2%	10%	1.3%↓	97.7%	100%	44.8%↓	0%	0%	8.4%↓	0%	0%
	Adi [18]	8.4%↓	4.3%	40%	1.9%↓	88.7%	100%	45.7%↓	4.1%	45%	4.8%↓	5.4%	65%
	Zhang [20]	8.5%↓	0.7%	0%	1.8%↓	63.9%	100%	47.4%↓	0.0%	0%	4.8%↓	1.6%	20%
Caltech-101	IWE (ours)	2.5%↓	90.5%	95%	0.3%↓	92.4%	100%	/			1.6%↓	92.3%	100%
	EWE [21]	2.7%↑	11.9%	75%	1.9%↑	23.2%	90%				5.2%↑	18.0%	35%
	Bansal ^{wb} [17]	2.4%↓	1.78%	50%	0.1%↑	26.0%	100%				1.9%↓	41.8%	100%
	Bansal ^{bb} [17]	2.4%↓	76.9%	100%	0.1%↑	100.0%	100%				1.9%↓	92.5%	100%
	Adi [18]	3.5%↓	53.7%	75%	0.4%↓	98.0%	100%				1.7%↓	4.7%	50%
	Zhang [20]	3.7%↓	73.9%	80%	0.4%↓	100.0%	100%				1.6%↓	46.2%	55%

Fine-Prune (FP) [27] prune 99% neurons in the last convolutional layer, while Adversarial neuron prune (ANP) [29] prune 20% of neurons in all layers. ANP’s applicability to Caltech101 is restricted by its attack setting; refer to the experiment setup for details. The notations Bansal^{wb} and Bansal^{bb} distinguish between their white-box and black-box verification implementations.

recently in privacy community [47] and is suggested to provide a more systematic comparison than other heuristic metrics.

A watermarking scheme is said to be strong if its ACC is close to that of clean models while achieving a $\text{TPR}@5\%\text{FPR}$ close to 100% when under attacks. Equivalently, a watermark embedding scheme is considered strong if no attack can reduce $\text{TPR}@5\%\text{FPR}$ without significantly compromising ACC.

C. Main Results

We assess the fidelity and robustness of the proposed IWE method on the three datasets mentioned. The results of fidelity and robustness are presented in Tables IV and V respectively. All results were derived from 20 independent runs.

Fidelity of IWE. We first study the performance drop in different watermark embedding methods. Table IV compares the main task accuracy (ACC) across different watermark embedding schemes. Notably, the ACC of the proposed IWE method is very close to that of a clean model, indicating negligible performance degradation in IWE. This success may be attributed to the synergistic effects of our logit reusing scheme and the design of the watermark task: the former minimizes the potential conflict between the main and watermark tasks, while the latter introduce additional augmented samples in training, which promotes generalization.

Robustness of IWE. We next study the robustness of IWE against various adversaries. To demonstrate the robustness of IWE, we visualize the distributions of $\text{ACC}_W(f)$ for both clean models and IWE watermarked models when being attacked in Fig. 4. A significant separation between the distributions

of clean models and watermarked models indicates a strong defense against a specific attack. The figure clearly shows that it is easy to distinguish between clean and IWE watermarked models, that no attack can close the gap between the two populations, suggesting that IWE a strong defense against the various attacks.

In Table V, we further provide a detailed, case-by-case analysis for each of the attack considered, where we compare the proposed IWE method with baseline methods. In particular:

- *Fine-tuning (FT) Attack.* This attack involves initially removing the watermark using a relatively large learning rate, followed by a repairing stage where one gradually restores the damaged functionality with smaller learning rates. Our method demonstrates robust defense against this attack, as evidenced by the high True Positive Rates (TPRs) reported in Table V. EWE [21] and Bansal^{wb} [17] are the next best performing methods in this attack scenario, although they are only effective on two of the three datasets. Other methods struggle to maintain a high TPR under this attack. We attribute the success of our method to the entanglement of the main and watermark tasks, which helps safeguard the watermark from being easily removed during fine-tuning.
- *Fine-pruning (FP) attack.* This white-box attack attempts to remove the watermark by deleting specific neurons in the last convolutional layer of the network. Our results in Table V indicate that this approach is also ineffective against the proposed IWE method. A more in-depth analysis is shown in Fig. 5.(a) and Fig. 5.(b). It can be seen from the figures that as more neurons are pruned from the model, both the watermark accuracy and the main task accuracy decline

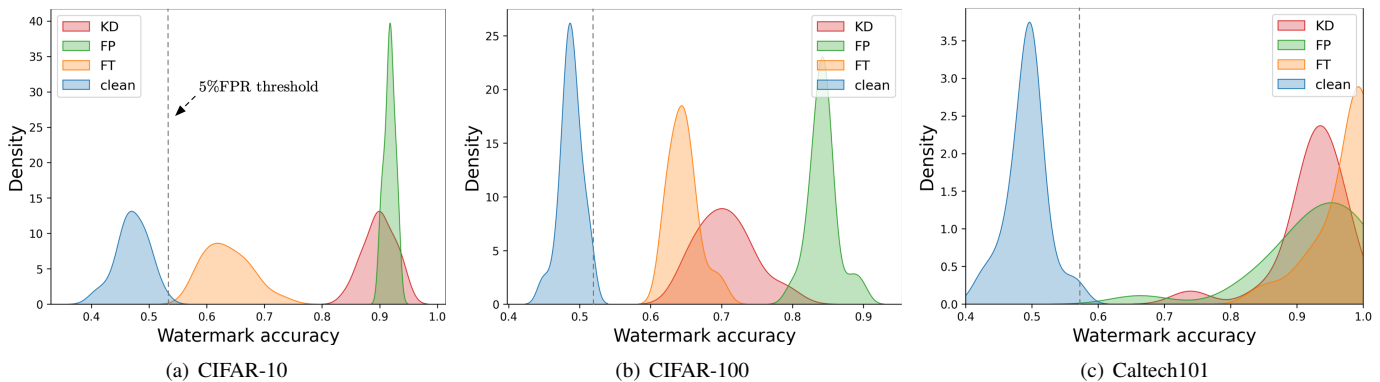


Fig. 4: The distribution of watermark accuracy (i.e., ACC_W) for clean model and IWE watermarked model. The curve ‘Clean’ represents the case of a clean model (i.e., no watermark) and the other curves represent the cases when a IWE watermarked model is under attack. A large separation between the curves in the two cases indicates a strong defense. The dotted vertical line represents the threshold t in Algorithm 2, which corresponds to a significance level of 5% (so that $FPR = 5\%$).

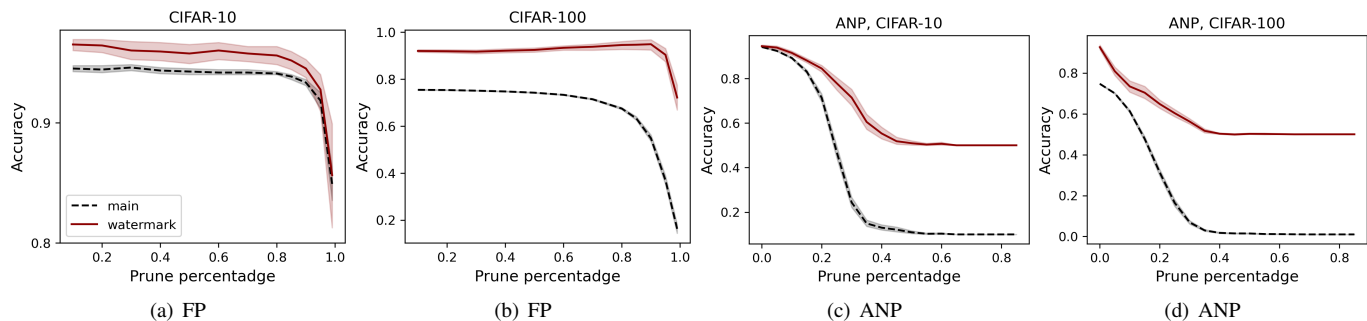


Fig. 5: Main task accuracy and watermark accuracy as a function of the percentage of pruned neurons in proposed IWE method. (a) and (b) show the cases for the fine-pruning (FP) attack [27] whereas (c) and (d) show the case for the adversarial neuron pruning (ANP) attack [29]. As more neurons are pruned, the main task accuracy and the watermark accuracy drops simultaneously, suggesting that the neurons used by the two tasks largely overlap with each other.

concurrently. This suggests that any attempts to remove the watermark by deleting neurons in IWE-protected model will inevitably compromises accuracy, being ineffective in attack.

- *Adversarial neuron pruning (ANP)*. Unlike the FP attack, which only targets neurons in the last convolutional layer, this attack considers neurons across all layers, making it inherently a stronger attack. In fact, we find that ANP does more effectively reduce the watermark accuracy of the IWE method than FP, as illustrated in Fig. 5.(c) and Fig. 5.(d). Despite being a stronger attack, ANP remain unsuccessful to break our defense. For instance, when 20% of the neurons are pruned on CIFAR-100, the main task accuracy decreases by 60.7%, yet the True Positive Rate (TPR) of our method remains at 100%. Among the baseline methods, only the white-box Bansal^{wb} method shows a resilience comparable to ours against ANP, though it requires significantly longer execution time than our method; see Fig. 6. Note that we have not included results for Caltech101 in this analysis, as ANP is not applicable to cases involving pretrained models, which require modifying the structure of the model.
- *Knowledge distillation (KD) attack*. In addition to evaluating IWE’s effectiveness against white-box attacks, we also assess

its resilience to black-box adversaries, specifically the soft-label KD attack [35]. Results are detailed in the rightmost column of Table V. The settings for this attack are identical to the well-known distillation attacks [35], which is proven effective in removing watermarks for a broad array of models. Our findings demonstrate that IWE indeed provides superior defense against this kind of attack compared to baseline methods. For instance, in the case of CIFAR-10, KD fails to remove the watermark in IWE despite a 5.4% drop in ACC, while a similar reduction is already sufficient to compromise EWE [21].

Neuron sharing. Using in-distribution samples to construct the trigger set naturally promotes the defense against watermark erasure attacks. Thanks to the similarity between normal and trigger set samples, the neurons activated by these two kinds of samples will largely overlap with each other — a phenomena we call neuron sharing, see Fig. 2 for proof. As a result, any attempt to deactivate neurons in one task will inevitably deactivate neurons in the other task. This causes any attempts to erase watermark inevitably affect main task performance. This is evidenced by Fig. 5, where we visualize how the model’s performance changes w.r.t the number of pruned neurons in FP and ANP. Notably, as more neurons are pruned, both the main

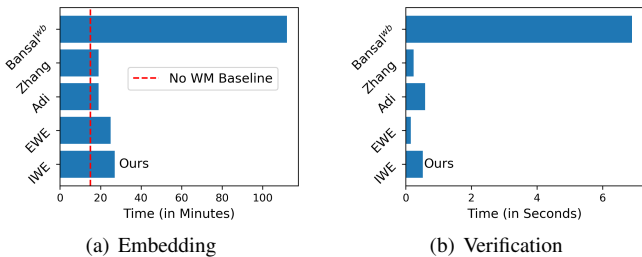


Fig. 6: Comparison of watermark embedding and verification execution time. A shorter time indicates a better efficiency.

task and watermark task performance exhibit similar declines. This suggests that neurons important for one task are also important for the other task, verifying our hypothesis.

D. Further Results

In this section, we provide further experimental results as well as related discussion about the proposed IWE method.

Execution time comparison. We compare the computation time of IWE with other baselines in Fig. 6. As shown in the figure, the computational time of our method is significantly lower than white-box methods, e.g., Bansal^{wb} [17]. These white-box methods typically require manipulating and checking the weights or the gradients of the network, which is computationally expensive compared to our method where access to the model outputs (the logits) are required. On the other hand, although our method the execution time of IWE is slightly higher than that of other black-box methods (e.g. EWE [21]), the gap is indeed small, especially considering that our method offers a much stronger defense against attacks.

FT Attack with other hyper-parameters. In the experiments, we find that the attack performance of fine-tuning attack (the REFIT attack [28]) depends on the initial learning rate η setting on the schedule, with larger η being more effective in removing watermarks but damaging more main task performance (and vice versa). We therefore conduct ablation studies with various η to thoroughly investigate the performance of the proposed IWE method under different attack setups. The results are shown in Fig. 7. Each data point in the figure corresponds to a specific choice of η . From the figure, it is clear that there is no way to remove watermark in the proposed IWE method without sacrificing performance, as can be seen from the positive correlation between accuracy and TPR. This however is not the case for EWE [21], where the adversary can easily reduce TPR without damaging main task accuracy by using a larger learning rate; see Fig. 7.(a). On CIFAR-100, it becomes relatively difficult to erase the watermark in EWE, yet the watermark in IWE is even more challenging to remove. The results suggest that the watermark embedded by IWE are more robust than EWE in all learning rate settings.

KD attack with other hyper-parameters. Apart from the default hyper-parameter settings [35] ($\tau = 10$, $\lambda = 1$) shown in Table V, we further explore other settings of hyper-parameter to thoroughly study IWE’s robustness against this attack. The results are shown in Table VI. Overall, we see that no KD

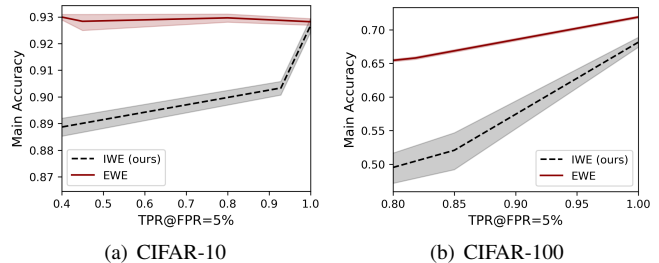


Fig. 7: Comparison of fine-tune attack resilience between IWE and EWE [21]. A steeper curve indicates a stronger defense.

settings can reduce $\text{TPR}@5\%\text{FPR}$ without a significant drop in ACC. An ACC drop of 4%-20% is typically required to remove the watermark in the proposed method. The results also suggest that hard label KD is ineffective for model theft under our protection scheme. Specifically, consider the setting $\tau = 1$, $\lambda = 0$ in Table VI. The main task accuracy (i.e., ACC) of hard label KD is clearly upper bounded by this configuration, as it can utilize more information from the logits than hard label KD. Given that this specific setting fails to achieve a reasonably good ACC, the same limitation also applies to hard label KD, rendering it ineffective.

VIII. CONCLUSION AND DISCUSSION

In this work, we introduce the In-distribution Watermark Embedding (IWE) as a novel approach to safeguarding the intellectual property of machine learning models. Our key finding is that existing backdoor-based watermark embedding schemes are inherently vulnerable to watermark erasure attacks due to their reliance on outlier trigger set samples—a fundamental issue not readily resolved by algorithmic tweaks. To address this issue, we developed a new scheme using in-distribution samples, where we carefully select triggers from a modified pool of normal samples. This approach encourages the strong entanglement between the main prediction task and the embedded watermarks, rendering any attempt to remove the watermark detrimental to performance. Additionally, our analysis of the role of logits as watermark information carrier has led to the innovative technique of redundant logits reusing, a technique designed to minimize the conflict between the watermark task and the main task. Experiments on three real-world datasets against diverse attacks including model fine-tuning, knowledge distillation, and network pruning fully demonstrate the effectiveness of the proposed method. To the best of our knowledge, we are the first to offer a robust defense against both white-box and black-box attacks with negligible performance impact, while without inspection of model parameters.

Our work also reveals a crucial connection between model watermarking and membership inference attacks (MIA). MIA [39] reveal that the logits of a model can contain rich information that is well beyond just class labels, such as the membership of a specific sample in dataset. While MIA use logits information to attack data privacy, we use logits information to carry watermarks and verify the ownership of a model, where a strong membership in a secret dataset proves

TABLE VI: IWE robustness against other KD attack settings.

Dataset	KD ($\lambda = 0, \tau = 1$) †			KD ($\lambda = 1, \tau = 2$)			KD ($\lambda = 1, \tau = 10$)		
	Δ ACC	ACC _W	TPR@5%FPR	Δ ACC	ACC _W	TPR@5%FPR	Δ ACC	ACC _W	TPR@5%FPR
CIFAR-10	10.5%↓	66.9%	100%	9.0%↓	75.3%	100%	4.6%↓	89.9%	100%
CIFAR-100	20.3%↓	55.2%	40%	15.6%↓	66.1%	100%	7.1%↓	70.6%	100%
Caltech101	3.7%↓	56.8%	60%	2.0%↓	80.2%	100%	1.6%↓	92.3%	100%

† The setting KD ($\lambda = 0, \tau = 1$) corresponds to model extraction attack [7]. Here, τ controls the smoothness of the teacher’s output distributions, where a larger τ results in smoother distributions and typically better distillation performance. λ balances the contribution of ground-truth labels and teacher predictions in knowledge distillation, with $\lambda = 0$ indicating no ground-truth labels are used.

ownership. This exploration bridges the two research areas of MIA and model ownership protection which were thought to be orthogonal, offering new insights to the research community.

Despite our powerful watermarking method, we note that our method is not a silver bullet. For example, our method is not so suitable for the case where the model is completely a black-box, e.g., the model stealer hides behind a cloud-based API and refuses to provide the details of the model (strictly speaking, our method only needs to check the model’s computational graph rather than the full model parameters, yet it is still beyond black-box access). In such case, the stealer may obfuscate the watermark information by returning fake logits during ownership verification, causing verification unsuccessful. Nevertheless, we note that this is a necessary cost of being robust to watermark erasure attack, as the model prediction (i.e. the predicted class label) itself is insufficient to carry watermark information; see our analysis in Section VI-B. Exploring more robust methods for embedding watermark information in the logits is an important future research direction.

In the future, we plan to extend the application of IWE to other data modality such as tabular data and speech signals, leveraging the information-theoretic insights unveiled in this research. The construction of in-distribution trigger sets within these contexts may present an intriguing area of exploration. Another direction worth exploring is the adaption of our method to generative AI models, such as large language models (LLMs) [10], [48]–[50]. While watermarking LLMs may be inherently more complex, they can essentially be viewed as classifiers that predict the next token based on the current ones. Thus, the insights and techniques developed in this work may naturally be transferable to the domain of LLMs. We leave the exploration of this exciting direction to future works.

REFERENCES

- [1] J. Devlin, M.-W. Chang, K. Lee, and K. Toutanova, “BERT: Pre-training of deep bidirectional transformers for language understanding,” *arXiv*, May 2019.
- [2] A. Radford, J. Wu, R. Child, D. Luan, D. Amodei, I. Sutskever *et al.*, “Language models are unsupervised multitask learners,” *OpenAI blog*, vol. 1, no. 8, p. 9, 2019.
- [3] T. Brown, B. Mann, N. Ryder, M. Subbiah, J. D. Kaplan, P. Dhariwal, A. Neelakantan, P. Shyam, G. Sastry, A. Askell *et al.*, “Language models are few-shot learners,” in *Proceedings of the Advances in neural information processing systems*, vol. 33, 2020, pp. 1877–1901.
- [4] H. Jia, M. Yaghini, C. A. Choquette-Choo, N. Dullerud, A. Thudi, V. Chandrasekaran, and N. Papernot, “Proof-of-learning: Definitions and practice,” in *Proc. IEEE Symp. Secur. Priv. (SP)*. IEEE, 2021, pp. 1039–1056.
- [5] L. Fan, K. W. Ng, C. S. Chan, and Q. Yang, “Deepip: Deep neural network intellectual property protection with passports,” *IEEE Trans. Pattern Anal. Mach. Intell.*, no. 01, pp. 1–1, 2021.
- [6] J. Guo, Y. Li, L. Wang, S.-T. Xia, H. Huang, C. Liu, and B. Li, “Domain watermark: Effective and harmless dataset copyright protection is closed at hand,” *Advances in Neural Information Processing Systems*, vol. 36, 2024.
- [7] F. Tramèr, F. Zhang, A. Juels, M. K. Reiter, and T. Ristenpart, “Stealing machine learning models via prediction apis,” in *Proceedings of the 25 USENIX Conference on Security Symposium*, 2016, pp. 601–618.
- [8] T. Orekondy, B. Schiele, and M. Fritz, “Knockoff nets: Stealing functionality of black-box models,” in *Proceedings of the IEEE/CVF conference on computer vision and pattern recognition*, Jun 2019, pp. 4949–4958.
- [9] M. Jagielski, N. Carlini, D. Berthelot, A. Kurakin, and N. Papernot, “High accuracy and high fidelity extraction of neural networks,” in *Proceedings of the 29th USENIX Conference on Security Symposium*, 2020, pp. 1345–1362.
- [10] J. Kirchenbauer, J. Geiping, Y. Wen, J. Katz, I. Miers, and T. Goldstein, “A watermark for large language models,” in *Proc. Int. Conf. Mach. Learn. (ICML)*. PMLR, 2023, pp. 17 061–17 084.
- [11] Y. Zhao, T. Pang, C. Du, X. Yang, N.-M. Cheung, and M. Lin, “A recipe for watermarking diffusion models,” *arXiv*, 2023.
- [12] N. Yu, V. Skripniuk, S. Abdelnabi, and M. Fritz, “Artificial fingerprinting for generative models: Rooting deepfake attribution in training data,” in *Proc. IEEE/CVF Int. Conf. Comput. Vis. (ICCV)*, 2021, pp. 14 448–14 457.
- [13] I. Cox, M. Miller, J. Bloom, and C. Honsinger, “Digital watermarking,” *J. Electron. Imaging*, vol. 11, no. 3, pp. 414–414, 2002.
- [14] F. Hartung and M. Kutter, “Multimedia watermarking techniques,” *Proc. IEEE*, vol. 87, no. 7, pp. 1079–1107, 1999.
- [15] Y. Uchida, Y. Nagai, S. Sakazawa, and S. Satoh, “Embedding watermarks into deep neural networks,” in *Proc. 2017 ACM Int. Conf. Multimedia Retrieval*, Jun 2017, pp. 269–277.
- [16] B. D. Rouhani, H. Chen, and F. Koushanfar, “Deepsigns: A generic watermarking framework for ip protection of deep learning models,” in *Proc. 24th Int. Conf. Archit. Support Program. Lang. Oper. Syst. (ASPLOS)*, Apr 2019, pp. 485–497.
- [17] A. Bansal, P. Chiang, M. J. Curry, R. Jain, C. Wigington, V. Manjunatha, J. P. Dickerson, and T. Goldstein, “Certified neural network watermarks with randomized smoothing,” in *Proc. Int. Conf. Mach. Learn. (ICML)*. PMLR, 2022, pp. 1450–1465.
- [18] Y. Adi, C. Baum, M. Cisse, J. Keshet, and B. Pinkas, “Turning your weakness into a strength: Watermarking deep neural networks by backdooring,” in *Proc. USENIX Secur. Symp.*, Aug 2018, pp. 1615–1631.
- [19] E. L. Merrer, P. Pérez, and G. Trédan, “Adversarial frontier stitching for remote neural network watermarking,” *Neural Comput. Appl.*, vol. 32, no. 13, pp. 9233–9244, 2020.
- [20] J. Zhang, Z. Gu, J. Jang, H. Wu, M. P. Stoeklin, H. Huang, and I. Molloy, “Protecting intellectual property of deep neural networks with watermarking,” in *Proc. 2018 Asia Conf. Comput. Commun. Secur.*, May 2018, pp. 159–172.
- [21] H. Jia, C. A. Choquette-Choo, V. Chandrasekaran, and N. Papernot, “Entangled watermarks as a defense against model extraction,” in *Proc. 30th USENIX Secur. Symp. (USENIX Secur. 21)*, Aug 2021, pp. 1937–1954.
- [22] R. Namba and J. Sakuma, “Robust watermarking of neural network with exponential weighting,” in *Proc. 2019 ACM Asia Conf. Comput. Commun. Secur.*, 2019, pp. 228–240.
- [23] S. Szyller, B. G. Atli, S. Marchal, and N. Asokan, “Dawn: Dynamic adversarial watermarking of neural networks,” in *Proc. 29th ACM Int. Conf. Multimedia*, 2021, pp. 4417–4425.
- [24] L. Fan, K. W. Ng, and C. S. Chan, “Rethinking deep neural network ownership verification: Embedding passports to defeat ambiguity attacks,” *Adv. Neural Inf. Process. Syst.*, vol. 32, 2019.
- [25] Y. Li, Y. Jiang, Z. Li, and S.-T. Xia, “Backdoor learning: A survey,” *IEEE Trans. Neural Netw. Learn. Syst.*, vol. 35, no. 1, pp. 5–22, 2024.

- [26] A. Saha, A. Subramanya, and H. Pirsiavash, "Hidden trigger backdoor attacks," in *Proc. AAAI Conf. Artif. Intell.*, vol. 34, no. 07, 2020, pp. 11 957–11 965.
- [27] K. Liu, B. Dolan-Gavitt, and S. Garg, "Fine-pruning: Defending against backdooring attacks on deep neural networks," in *Proc. Res. Attacks, Intrusions, Defenses (RAID)*, 2018, pp. 273–294.
- [28] X. Chen, W. Wang, C. Bender, Y. Ding, R. Jia, B. Li, and D. Song, "REFIT: A unified watermark removal framework for deep learning systems with limited data," in *Proc. 2021 ACM Asia Conf. Comput. Commun. Secur.*, May 2021, pp. 321–335.
- [29] D. Wu and Y. Wang, "Adversarial neuron pruning purifies backdoored deep models," *Adv. Neural Inf. Process. Syst.*, vol. 34, pp. 16 913–16 925, 2021.
- [30] Y. Li, X. Lyu, X. Ma, N. Koren, L. Lyu, B. Li, and Y.-G. Jiang, "Reconstructive neuron pruning for backdoor defense," in *International Conference on Machine Learning*. PMLR, 2023, pp. 19 837–19 854.
- [31] D. Hitaj and L. V. Mancini, "Have you stolen my model? evasion attacks against deep neural network watermarking techniques," *arXiv*, Sep. 2018.
- [32] F. Boenisch, "A systematic review on model watermarking for neural networks," *Front. Big Data*, vol. 4, p. 729663, 2021.
- [33] B. Wang, Y. Yao, S. Shan, H. Li, B. Viswanath, H. Zheng, and B. Y. Zhao, "Neural cleanse: Identifying and mitigating backdoor attacks in neural networks," in *Proc. IEEE Symp. Secur. Priv. (SP)*. IEEE, 2019, pp. 707–723.
- [34] Y. Li, X. Lyu, N. Koren, L. Lyu, B. Li, and X. Ma, "Neural attention distillation: Erasing backdoor triggers from deep neural networks," in *Proceedings of the 9th International Conference on Learning Representations, ICLR 2021*, 2021.
- [35] Z. Yang, H. Dang, and E.-C. Chang, "Effectiveness of distillation attack and countermeasure on neural network watermarking," *arXiv*, Jun. 2019.
- [36] Y. Li, L. Zhu, X. Jia, Y. Jiang, S.-T. Xia, and X. Cao, "Defending against model stealing via verifying embedded external features," in *Proceedings of the AAAI Conference on Artificial Intelligence*, no. 2, 2022, pp. 1464–1472.
- [37] N. Lukas, E. Jiang, X. Li, and F. Kerschbaum, "Sok: How robust is image classification deep neural network watermarking?" in *2022 IEEE Symposium on Security and Privacy (SP)*. IEEE, 2022, pp. 787–804.
- [38] Y. Chen, D. Zhang, M. Gutmann, A. Courville, and Z. Zhu, "Neural approximate sufficient statistics for implicit models," *arXiv*, 2020.
- [39] R. Shokri, M. Stronati, C. Song, and V. Shmatikov, "Membership inference attacks against machine learning models," in *2017 IEEE Symposium on Security and Privacy (SP)*. IEEE, 2017, pp. 3–18.
- [40] T. Chen, S. Kornblith, M. Norouzi, and G. Hinton, "A simple framework for contrastive learning of visual representations," in *Proc. 37th Int. Conf. Mach. Learn. (ICML)*, ser. ICML '20, 2020.
- [41] Y. Li, L. Zhu, X. Jia, Y. Jiang, S.-T. Xia, and X. Cao, "Defending against model stealing via verifying embedded external features," vol. 36, no. 2, pp. 1464–1472. [Online]. Available: <https://ojs.aaai.org/index.php/AAAI/article/view/20036>
- [42] L. Fei-Fei, R. Fergus, and P. Perona, "One-shot learning of object categories," *IEEE Trans. Pattern Anal. Mach. Intell.*, vol. 28, no. 4, pp. 594–611, 2006.
- [43] P. Maini, M. Yaghini, and N. Papernot, "Dataset inference: Ownership resolution in machine learning," in *Proc. Int. Conf. Learn. Represent. (ICLR)*, 2020.
- [44] A. Hu, Z. Lu, R. Xie, and M. Xue, "Veridip: Verifying ownership of deep neural networks through privacy leakage fingerprints," *IEEE Transactions on Dependable and Secure Computing*, 2023.
- [45] Z. Peng, S. Li, G. Chen, C. Zhang, H. Zhu, and M. Xue, "Fingerprinting deep neural networks globally via universal adversarial perturbations," in *Proc. IEEE/CVF Conf. Comput. Vis. Pattern Recognit. (CVPR)*, 2022, pp. 13 430–13 439.
- [46] A. Bansal, P. Y. Chiang, M. J. Curry, R. Jain, C. Wiggington, V. Manjunatha, J. P. Dickerson, and T. Goldstein, "Certified neural network watermarks with randomized smoothing," in *Proc. 39th Int. Conf. Mach. Learn. (ICML)*, Jul 2022, pp. 1450–1465.
- [47] N. Carlini, J. Hayes, M. Nasr, M. Jagielski, V. Schwag, F. Tramèr, B. Balle, D. Ippolito, and E. Wallace, "Extracting training data from diffusion models," in *Proc. 32th USENIX Secur. Symp. (USENIX Secur. 23)*, 2023, pp. 5253–5270.
- [48] L. Pan, A. Liu, Z. He, Z. Gao, X. Zhao, Y. Lu, B. Zhou, S. Liu, X. Hu, L. Wen *et al.*, "Markllm: An open-source toolkit for llm watermarking," *arXiv preprint arXiv:2405.10051*, 2024.
- [49] M. Christ, S. Gunn, and O. Zamir, "Undetectable watermarks for language models," *arXiv preprint arXiv:2306.09194*, 2023.
- [50] K. Greshake, S. Abdelnabi, S. Mishra, C. Endres, T. Holz, and M. Fritz, "Not what you've signed up for: Compromising real-world llm-integrated applications with indirect prompt injection," in *Proceedings of the 16th ACM Workshop on Artificial Intelligence and Security*, 2023, pp. 79–90.